APPLIED AND ENVIRONMENTAL MICROBIOLOGY, Nov. 1999, p. 5107–5116 Vol. 65, No. 11
0099-2240/99/$04.00+0

Analyses of Spatial Distributions of Sulfate-Reducing Bacteria and Their Activity in Aerobic Wastewater Biofilms

SATOSHI OKABE,* TSUKASA ITOH, HISASHI SATOH, AND YOSHIMASA WATANABE

Department of Urban and Environmental Engineering, Graduate School of Engineering, Hokkaido University, Kita-ku, Sapporo 060-0813, Japan

Received 3 May 1999/Accepted 27 August 1999

The vertical distribution of sulfate-reducing bacteria (SRB) in aerobic wastewater biofilms grown on rotating disk reactors was investigated by fluorescent in situ hybridization (FISH) with 16S rRNA-targeted oligonucleotide probes. To correlate the vertical distribution of SRB populations with their activity, the microprofiles of O_2, H_2S, NO_2^-, NO_3^-, NH_4^+, and pH were measured with microelectrodes. In addition, a cross-evaluation of the FISH and microelectrode analyses was performed by comparing them with culture-based approaches and biogeochemical measurements. In situ hybridization revealed that a relatively high abundance of the probe SRB385-stained cells (approximately 10^9 to 10^{10} cells per cm^3 of biofilm) were evenly distributed throughout the biofilm, even in the oxic surface. The probe SRB660-stained *Desulfobulbus* spp. were found to be numerically important members of SRB populations (approximately 10^8 to 10^9 cells per cm^3). The result of microelectrode measurements showed that a high sulfate-reducing activity was found in a narrow anaerobic zone located about 150 to 300 μm below the biofilm surface and above which an intensive sulfide oxidation zone was found. The biogeochemical measurements showed that elemental sulfur (S^0) was an important intermediate of the sulfide reoxidation in such thin wastewater biofilms (approximately 1,500 μm), which accounted for about 75% of the total S pool in the biofilm. The contribution of an internal Fe-sulfur cycle to the overall sulfur cycle in aerobic wastewater biofilms was insignificant (less than 1%) due to the relatively high sulfate reduction rate.

Wastewater biofilms are very complex multispecies biofilms, displaying considerable heterogeneity with respect to both the microorganisms present and their physicochemical microenvironments. Moreover, multiple electron donors and electron acceptors are present in the wastewaters. Therefore, successive vertical zonations of predominant respiratory processes occurring simultaneously in close proximity have been found in aerobic wastewater biofilms with a typical thickness of only a few millimeters (10, 22, 40, 42). In these studies, sulfate reduction was found in the deeper anaerobic biofilm strata, even though the bulk liquid was oxygenated. Accordingly, reoxidation of the produced sulfide with oxygen and/or nitrate was found in a stratum close to the sulfate reduction zone, depending on the oxygen and nitrate penetration depths.

A major drawback of sulfate reduction in wastewater treatments is the production of toxic H_2S, which is also a possible precursor of odorants and significantly enhances microbially mediated corrosion of treatment facilities (23, 24, 31, 37). Furthermore, sulfate reduction accounts for up to 50% of the mineralization of organic matter in aerobic wastewater treatment systems (22). Once sulfate reduction occurs in biofilms, internal sulfide reoxidation is expected to account for a substantial part of oxygen consumption (approximately up to 70%) (22, 32, 42). Therefore, the in situ detection of populations of sulfate-reducing bacteria (SRB) and their activity in wastewater biofilms is of great practical and scientific relevance. However, such studies have been hindered due to lack of analytical tools and the complexity of the internal sulfur cycle in aerobic biofilms. Since mass balance of sulfide or sulfate flux across a biofilm-liquid interface cannot describe sulfur transformations within the biofilm, the sulfur cycle in wastewater biofilm systems is not well known presently.

Therefore, we must explore analytical tools to overcome this problem. Microelectrode measurements are the most reliable way of studying several metabolic processes with high spatial and temporal resolution and have been used for studying nitrogen cycles (11, 14, 36, 43, 44) and sulfur cycles (22, 40, 42) in various environmental samples. One advantage of the use of microelectrodes is their ability to detect in situ microbial activities with minimal disturbance. Furthermore, the recent development of the fluorescent in situ hybridization (FISH) technique with oligonucleotide probes has been widely used to study microbial community structures in microbial flocs (44, 47, 48) and biofilms (3, 36, 40, 43). FISH has been successfully combined with microelectrode measurements (36, 40, 43, 44). However, so far, studies relating in situ spatial distribution of SRB populations to their activity in wastewater biofilms are scarce.

In the present study, we combined three techniques to determine the vertical distribution of SRB populations, substrate profiles, and distributions of sulfur pools (i.e., S^0, FeS, and FeS_2) within aerobic wastewater biofilms. Firstly, the vertical distributions of SRB populations were investigated by FISH with the previously published phylogenetic probes in combination with confocal scanning laser microscopy (CSLM). This was done by counting positively probe-stained cells in vertical transects across biofilm sections. Secondly, the spatial distributions of in situ activities of sulfate reduction and sulfide oxidation were measured by means of several microelectrodes. The resulting picture was cross-evaluated with reference to one-dimensional vertical distributions of most-probable-number (MPN) counts of SRB populations and potential sulfate reduction rates (SRRs) and sulfide oxidation rates (SORs) in the biofilm, which were measured by slicing the biofilm parallel to the substratum without any pretreatment by the Microslicer (model DTK-1000; Dosaka EM Co., Ltd., Kyoto, Japan). Fi-

* Corresponding author. Mailing address: Department of Urban and Environmental Engineering, Graduate School of Engineering, Hokkaido University, North 13, West 8, Kita-ku, Sapporo 060-0813, Japan. Phone: 81-(0)11-706-6267. Fax: 81-(0)11-706-7890. E-mail: sokabe@eng.hokudai.ac.jp.

nally, a complementary analysis of sulfur compound (i.e., S^0, FeS, and FeS_2) distributions was performed to evaluate the importance and contribution of an internal iron-sulfur cycle in the overall sulfur cycle. The combination of these three techniques provides more comprehensive information on a complex sulfur cycle occurring in the aerobic wastewater biofilms.

MATERIALS AND METHODS

Biofilm samples. Aerobic mixed-population biofilms were grown in fully submerged rotating disk reactors (RDR) consisting of 10 polymethyl-methacrylate disks. Eight removable slides (1 by 6 cm) were installed in each disk for sampling biofilms. The reactor volume was 5,600 cm^3, and the total biofilm area was 4,020 cm^2. Disk rotational speed for 16-cm-diameter disks was fixed at 14 rpm (which gives a peripheral speed of ca. 14 cm s^{-1}). The dilution rate in the reactors was kept at 0.2 h^{-1}. The average dissolved organic carbon (DOC) loading rate was 11.2 g of DOC $(m^2$ of biofilm$)^{-1}$ h^{-1}. The primary settling tank effluent from the Soseigawa municipal wastewater treatment plant in Sapporo, Japan, consisting of stage 1 (215,000 population equivalents [PE] [1 PE = 60 g of biological oxygen demand day^{-1}]) and stage 2 (210,000 PE) was fed into the reactor. To facilitate sulfide denitrification, the influent was supplemented with KNO_3 solution to give a final concentration of 350 μM NO_3^-. Since the bulk water was not aerated, the average dissolved oxygen (DO) concentration in the bulk water was 40 ± 30 μM during the experiment.

Vertical distributions of MPN counts and activity profiles. The biofilms collected from the RDR were sliced into 50- to 100-μm-thick sections parallel to the substratum without any pretreatment by means of the Microslicer as described previously (34) and then apportioned into samples representing four to six layers. The apportioned samples were homogenized and subjected to the enumeration of MPN counts and the measurement of potential SRRs and SORs.

SRB were enumerated by the five-tube multiple-dilution MPN method with Hungate-type test tubes after homogenization of the sectioned biofilm samples. The slightly modified Postgate medium B (37) containing sodium propionate (500 mg of C $liter^{-1}$) as the sole carbon and energy source was used for the MPN count. Black cultures were counted at least 1 month after incubation.

Potential SRR (indicated as H_2S production rate) was determined from a standard batch experiment. The homogenized biofilm sections (variable volume) were transferred to 100 ml of the anaerobic modified Postgate medium B (the same as the MPN count) in a serum vial (130 ml). The vials were sparged with N_2 gas for at least 5 min and subsequently sealed with butyl rubber stoppers and aluminum seals. The vials were incubated on a rotary shaker at 20°C in the dark. A culture without addition of carbon source was used as a control. At regular intervals, subsamples were withdrawn with a sterilized syringe and immediately added to 1% zinc acetate (ZnAC) solution for acid-volatile sulfide (AVS; H_2S and FeS) analysis. The AVS was measured colorimetrically by the methylene blue method (7). The AVS accumulation rates during the initial 48-h incubation were used to calculate the potential SRRs for each sample.

The potential aerobic sulfide oxidation rate (ASOR; indicated as SO_4^{2-} production rate) was determined by using a growth medium containing (millimolar concentrations in distilled water) NH_4Cl (3.6), KH_2PO_4 (0.9), $MgSO_4 \cdot 7H_2O$ (1.6), $NaHCO_3$ (104), $Na_2S_2O_3 \cdot 5H_2O$ (1.7), and trace metals (46) (pH 7.0). Thiosulfate was used as substrate, instead of sulfide, because it is difficult to obtain a constant sulfide concentration due to spontaneous chemical reaction of H_2S and O_2 and emission of H_2S to the air phase. For the determination of the potential anaerobic sulfide oxidation rate (ANSOR; indicated as SO_4^{2-} production rate), KNO_3 (3.6 mM) and $Na_2S \cdot 9H_2O$ (1.6 mM) instead of thiosulfate were used as the electron acceptor and donor, respectively. The biofilm samples were inoculated into 100 ml of the medium and incubated aerobically or anaerobically on a rotary shaker at 20°C in the dark. The medium without the inoculum was used as a control. At regular intervals, subsamples were withdrawn for SO_4^{2-} measurement. The concentration of SO_4^{2-} was analyzed with an ion chromatograph (model DX-100 with AS4A column; Nippon DIONEX, Osaka, Japan). Although the medium already contained 1.6 mM SO_4^{2-}, the aerobic and anaerobic H_2S oxidation activities were very high in this study, so that an increase in the SO_4^{2-} concentration could be measured with minimum errors.

Measurement of reduced sulfur compounds. Elemental sulfur (S^0), AVS (H_2S and FeS), and chromium-reducible sulfide (CRS; FeS_2) in biofilms were determined by the method described originally by Fossing and Jorgensen (18) and modified by Nielsen et al. (31). The biofilm samples were immediately fixed in 1% ZnAC solution, sliced into 50- to 100-μm-thick sections parallel to the substratum in 1% ZnAC solution without any prefixation by means of the Microslicer, and then apportioned into samples representing four to six layers. The apportioned biofilm samples were sequentially analyzed for elemental sulfur (S^0), AVS (H_2S and FeS), and CRS (FeS_2). Elemental sulfur was extracted with 96% ethanol for 24 h at room temperature prior to AVS and CRS measurements. Samples extracted in ethanol were analyzed by a high-performance liquid chromatograph (HPLC) with a UV detector at 254 nm. A reversed-phase column (Partisil 5; octyldecyl silane 3; Whatman) was used with 100% high-performance liquid chromatography-grade methanol as eluent and a flow rate of 0.4 ml min^{-1}. The sample injection volume was 100 μl. The remaining samples from ethanol extraction were suspended in 10 ml of 1% ZnAC solution, and AVS (H_2S and FeS) was volatilized by addition of 10 ml of 2 N HCl. The volatilized H_2S was trapped in 1% ZnAC solution (variable volumes) and measured colorimetrically by the methylene blue method (7). After the AVS distillation, 2.5 ml of 1 M Cr^{2+} in 0.5 N HCl solution was added directly to the remaining sample suspension from S^0 and AVS analyses. CRS was volatilized, and H_2S was measured as described above. Recovery of FeS and FeS_2 was determined to be (87 ± 7)% (n = 3) and (73 ± 24)% (n = 3), respectively.

Measurements of total Fe and total Mn contents in the biofilm. Biofilm samples were embedded in Tissue-Tek OCT compound (Miles, Elkhart, Ind.) and rapidly frozen at −20°C. Horizontal sections (40 μm thick) of the frozen biofilm (about 1 by 1 cm) were obtained parallel to the substratum by use of a cryostat (Reichert-Jung Cryocut 1800; Leica) and then apportioned into samples representing four to six layers. Each of the apportioned samples was transferred into an acid-cleaned test tube containing 6.5 N HNO_3 (5 ml) and ultrasonicated for 10 min. Total Fe and Mn concentrations were determined by the polarized Zeeman atomic adsorption spectrophotometer (model Z-5700; Hitachi, Tokyo, Japan) after appropriate dilutions of the samples were made.

Microelectrodes. Concentration profiles of O_2, NO_2^-, NO_3^-, pH, and H_2S in the biofilms were measured by microelectrodes manufactured in our laboratory. Cathode-type oxygen microelectrodes with a tip diameter of about 15 μm were prepared and calibrated as described previously by Revsbech and Jorgensen (41). Liquid ion-exchanging membrane microsensors for NH_4^+, NO_2^-, and NO_3^- were prepared as described before (10, 11, 13) and calibrated in a dilution series (10^{-3} to 10^{-6} M) of NH_4^+, NO_2^-, and NO_3^- in the medium used for the measurements. pH electrodes with tip diameters of about 5 to 10 μm were constructed according to the procedure of deBeer and van den Heuvel (12). The pH microelectrode was calibrated in the medium with an adjusted pH in the range of 4 to 9. The sulfide electrodes were manufactured as described by Revsbech and Jorgensen (41) and were calibrated as described by Kuhl and Jorgensen (22). The total sulfide concentration (H_2S, HS^-, and S^{2-}) in a dilution series was determined by the methylene blue method (7). The total amount of dissolved H_2S, HS^-, and S^{2-} is designated H_2S or total sulfide in the rest of the paper. The 90% response times were approximately 1 to 5 min, depending on sulfide concentration. Since the pH profiles showed a significant variation (>0.1 pH unit) throughout the biofilm, pH correction of the measured sulfide profiles was necessary. The total sulfide concentration in an aqueous solution can be calculated as described by Kuhl and Jorgensen (22). We used the following dissociation constants for sulfide, $pK_1 = 7.05$ and $pK_2 = 17.1$ (29).

Microelectrode measurements. Biofilms were taken from the reactors and incubated in the synthetic medium for about 3 h before measurements were made, which ensured steady-state concentration profiles. The medium contained the following (in micromolar concentrations): $NaNO_3$ (270), $NaNO_2$ (100), $MgSO_4 \cdot 7H_2O$ (300), sodium propionate (600), NH_4Cl (600), Na_2HPO_4 (570), $MgCl_2 \cdot 6H_2O$ (84), $CaCl_2$ (200), and EDTA · 2Na (270). All measurements were performed in a water chamber containing 1.8 liters of the synthetic medium at 20°C. Each microelectrode was separately mounted on a motor-driven micromanipulator (model ACV-104-HP; Chuo Precision Industrial Co., Ltd., Tokyo, Japan). The electrode assembly was placed inside a Faraday cage to reduce electrical noise. Each measurement was performed three to five times by advancing the electrodes at depth steps of 50 to 100 μm through the biofilm. Average liquid flow velocity (2 to 3 cm s^{-1}) above the biofilm was provided by a Pasteur pipette blowing a mixture of air and N_2 gas onto the water surface. The bulk DO concentration was kept the same as the one in the RDR. The biofilm-liquid interface was determined by using a dissection microscope (model Stemi 2000; Carl Zeiss).

Estimations of specific reaction rates and substrate flux. Net specific consumption and production rates (R; micromoles $centimeter^{-3}$ $hour^{-1}$) were estimated from the measured microprofiles by using Fick's second law of diffusion. The details of this method have been described previously by Lorenzen et al. (26). Furthermore, the total diffusion fluxes (J; micromoles $centimeter^{-2}$ $hour^{-1}$) through the biofilm-liquid interface were calculated by using Fick's first law, $J = -D_s$ (dS/dz), where D_s is the molecular diffusion coefficient of compound S in the biofilm and dS/dz is the concentration gradient in the boundary layer at the biofilm-liquid interface, which is determined from microprofiles. We used the molecular diffusion coefficients of 2.09×10^{-5} cm^2 s^{-1} for oxygen (4), 1.23×10^{-5} cm^2 s^{-1} for NO_3^- (4), and 1.39×10^{-5} cm^2 s^{-1} for sulfide (22) at 20°C.

Oligonucleotide probes. In situ hybridization of biofilm sections was performed with the following 16S rRNA-targeted oligonucleotide probes: (i) EUB338 (1), (ii) SRB385 (3, 39), (iii) SRB385Db (38), and (iv) four group-specific probes (SRB687, SRB660, SRB129, and SRB221) (15). All probe sequences, their specificities, hybridization conditions, and references are given in Table 1. All probes were synthesized and labeled with tetramethylrhodamine-5-isothiocyanate (TRITC) at the 5′ end by TaKaRa Shuzou Co., Ltd. (Shiga, Japan) (2).

FISH. Biofilm samples were fixed in 4% paraformaldehyde solution (2) immediately after the microelectrode measurements and embedded in Tissue-Tek OCT compound. Horizontal and vertical (cross section) thin sections (20 μm thick) of the fixed biofilm were prepared as described by Ramsing et al. (40). The previously published optimal hybridization conditions were used for each probe. All in situ hybridizations were performed according to the procedure described by Amann (1) in 8 μl of hybridization buffer (0.9 M NaCl, 20 mM Tris hydro-

TABLE 1. A list of 16S rRNA-targeted oligonucleotide probes used in this study

Probe	Specificity	Sequence of probe (5′-3′)	Target site[a]	FA[b] (%)	NaCl[c] (mM)	Reference(s)
EUB338	Domain *Bacteria*	GCTGCCTCCCGTAGGAGT	338–355	20	0.166	1
SRB385	SRB of the delta *Proteobacteria* plus several gram-positive bacteria (e.g., *Clostridium* spp.)	CGGCGTCGCTGCGTCAGG	385–402	30	0.071	3, 39
SRB385Db	Family *Desulfobacteriaceae* (except for *Desulfobulbus* spp.) plus some non-sulfate-reducing bacteria (e.g., *Myxococcus xanthus* and *Pelobacter acetylenicus*)	CGGCGTTGCTGCGTCAGG	385–402	30	0.071	38
SRB687	*Desulfovibrio* spp. plus members of the genera *Geobacter*, *Desulfomonas*, *Desulfuromonas*, *Desulfomicrobium*, *Bilophila*, and *Pelobacter*	TACGGATTTCACTCCT	687–702	10	0.386	15
SRB660	*Desulfobulbus* spp.	GAATTCCACTTTCCCCTCTG	660–679	30	0.071	15
SRB129	*Desulfobacterium* spp.	TGCGCGGACTCATCTTCAAA	221–240	10	0.386	15
SRB221	*Desulfobacter* spp.	CAGGCTTGAAGGCAGATT	129–146	20	0.166	15

[a] 16S rRNA position according to *Escherichia coli* numbering.
[b] Formamide concentration in the hybridization buffer.
[c] Sodium chloride concentration in the washing buffer.

chloride [pH 7.2], 0.01% sodium dodecyl sulfate; formamide concentrations are shown in Table 1) with 1 μl of probe solution at 46°C for 2 to 3 h in an equilibrated sealed moisture chamber. The final probe concentration was approximately 5 ng μl^{-1}. Subsequently, a stringent washing step was performed at 48°C for 20 min in 50 ml of prewarmed washing solution (NaCl concentration is shown in Table 1; 20 mM Tris hydrochloride [pH 7.2], 0.01% sodium dodecyl sulfate). The stringency of the washing step was adjusted by lowering the sodium chloride concentration to achieve the appropriate specificity. The slides were then rinsed briefly with ddH_2O, allowed to air dry, and mounted in antifading solution (Slow Fade Light; Molecular Probes, Eugene, Oreg.).

Microscopy. An LSM 510 CSLM (Carl Zeiss) equipped with an argon laser (488 nm) and a HeNe laser (543 nm) was used to examine the biofilm specimens. Zeiss filter sets 09 and 15 and ×20, ×40, and ×63 oil-immersion lenses were used. Wastewater biofilm samples generally contain detrital matters and mineral grains, which generate problems with autofluorescence and unspecific staining. These mineral grains and detrital matters generally exhibit a wide range of emission spectra. Thus, although biofilm samples were hybridized with only TRITC-labeled probes, images were recorded by using simultaneous excitation of 488- and 543-nm lasers. By doing this, only TRITC-labeled probe-stained cells appeared red, and other debris and mineral grains appeared yellowish due to dual excitation. In this way, the probe-stained cells could easily be distinguished from other materials. All image combining, processing, and analysis were performed with the standard software package provided by Zeiss. Processed images were printed out by using the software package Adobe Photoshop 3.0J (Adobe Systems Incorporated, Mountain View, Calif.).

Vertical distribution of SRB. To quantify the vertical distributions of SRB populations from FISH images, we directly counted positively probe-stained cells along vertical transects through the biofilm (40). In parallel, surface fractions of probe-stained cell area to total biomass area (differential interference contrast [DIC] image) were measured for the horizontal biofilm sections taken from representative depths of the biofilm. Three randomly chosen slices were stained with TRITC-labeled SRB385 probe, three were stained with TRITC-labeled SRB660 probe, and three were used as controls without staining. The nine slides were randomly mixed, and the positive cells along three vertical transects on each slide were counted without knowledge of the probe that had been used to stain the particular slide. The transects were made by counting the cells within a scan frame. The counts were recalculated to absolute cell density from the scan frame area and the scan depth.

The total biomass area and probe-stained area were measured from DIC images and CSLM projection images of the same microscopic field, respectively, by using image analysis software provided by Zeiss. At least five representative microscopic images of each horizontal section of the biofilm were analyzed at corresponding biofilm depths. Since fluorescence intensity derived from probe-stained cells varied slightly for each image, the highest fluorescence intensity of background was firstly determined. This value was used as a threshold low value. The threshold value used for the 543-nm channel was in the range of 30 to 50, depending on autofluorescence intensity (each colored pixel was assigned an intensity level from 0 to 255). Thus, all pixels with fluorescence intensity above the threshold value were counted as probe-stained area.

RESULTS

General biofilm reactor performance. Typical water quality in influent and effluent of the reactor after reaching the steady-state condition is shown in Table 2. The steady state was achieved after about 40 days. Relatively large standard deviations are attributed to fluctuations in the influent water quality. The average DO concentration in the bulk water was low (about 40 ± 30 μM) because of no aeration in the bulk water. Nitrification activity was not observed. Effluent SO_4^{2-} and NH_4^+ concentrations were not statistically different from those of the influent, indicating that sulfur transformation in the reactor could not be seen from mass balance on SO_4^{2-}. Consumption of nitrate indicated the occurrence of denitrification or reduction of nitrate to ammonium by SRB to a certain extent.

Biofilm architecture. The biofilm reactor had been at steady state for more than 1 month. Biofilm sloughing did not occur during this period. Figure 1 shows a composite cross-section (20-μm-thick) image of a 60-day-old wastewater biofilm (biofilm thickness, approximately 1,100 μm). It is clear that the wastewater biofilms studied have a complex heterogeneous structure consisting of discrete biomass (microbial aggregates) and interstitial voids, which connect the bulk water to the bottom part of the biofilm.

In situ detection of SRB. Immediately after the microelectrode measurements (the results are shown below), a series of vertical sections of the biofilm were subjected to in situ hybridization. Firstly, four group-specific probes were used to specify possible numerically predominant species of SRB populations in the biofilm. Only a few positive cells were found when

TABLE 2. Average influent and effluent water characteristics during an experimental period[a]

Characteristic	Influent	Effluent
SO_4^{2-}	290 (±60)	330 (±80)
NO_3^-	347 (±46)	13 (±10)
NH_4^+	677 (±220)	693 (±193)
DOC	1,560 (±530)	1,250 (±510)
Total Fe	54.5 (±11.5)	26.0 (±1.0)
Dissolved Fe	8.0 (±2.0)	10.1 (±3.0)
DO		40 (±30)
Temp (°C)		13.7 (±5.2)
pH		6.9 (±0.3)

[a] Data were collected after the steady-state condition was achieved. Values in parentheses are standard deviations. Except for temperature and pH, values are shown in micromoles $liter^{-1}$.

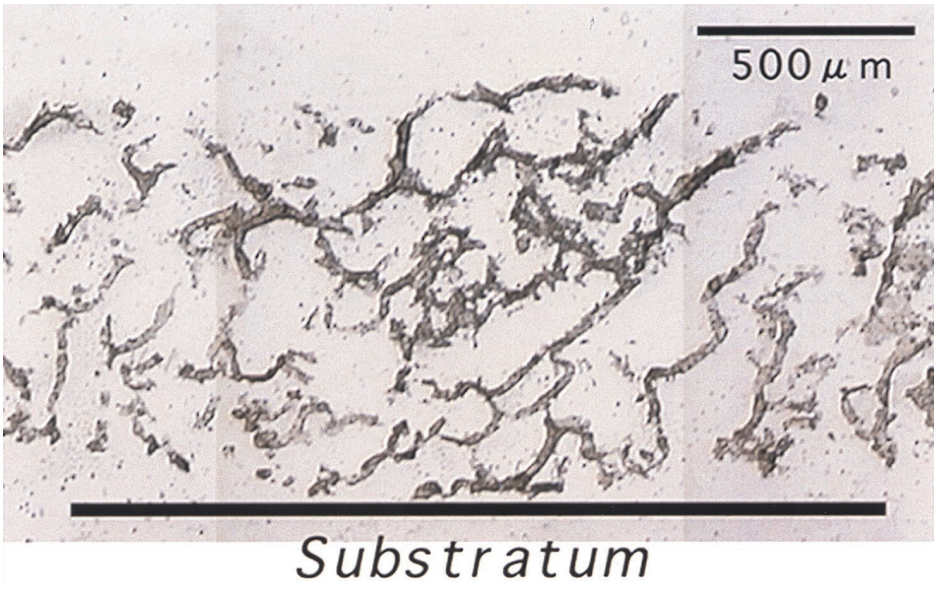

FIG. 1. A cross section made with a cryomicrotome (20 μm thick) of an aerobic domestic wastewater biofilm. The biofilm thickness is approximately 1,000 μm.

SRB129, SRB687, and SRB221 probes were used with any of the biofilm samples, and their fluorescence intensities were very low. An abundance of SRB660 probe-stained cells was found at all depths, and their fluorescence signals were strong. Based on these findings, *Desulfobulbus* spp. could be a numerically important member of SRB populations in this biofilm.

Figure 2A shows a composite cross-section DIC image to display the entire biofilm structure. The vertical biofilm sections revealed that the fluorescent signals derived from SRB660 probe-stained cells were found at all depths in all states from single scattered cells (Fig. 2B) to clustered cells (Fig. 2C). More clustered cells were found in the deeper part of the biofilm than in the surface biofilm. The SRB385 probe-stained cells formed rather irregular and relatively small clusters, consisting of up to a few hundred cells (Fig. 2D to G). Some of these cells display a lemon shape, and a few cells were linked together, which seem to be typical features of *Desulfobulbus* spp. (49).

Vertical distribution of SRB population. Figure 3A presents the vertical distributions of SRB385 and SRB660 probe-stained cells in the biofilm. The SRB385 probe-stained cells were present in high numbers (approximately $10 \times 10^9 \pm 1.6 \times 10^9$ cells cm^{-3}) and evenly distributed throughout the biofilm, even in the oxic zone. The vertical distribution of the SRB660 probe-stained cells also revealed that there was no significant difference between the average cell counts in the oxic zones and those in the anoxic zones of the biofilms, approximately 10^9 cells cm^{-3}. They accounted for about 6 to 23% of the SRB385 probe-stained cells. In addition, three slices of the samples at depths of approximately 200 and 900 μm hybridized with the SRB385Db probe. The numbers of SRB385Db probe-stained cells were approximately 0.7×10^9 cells cm^{-3} at depths of 200 and 900 μm, respectively, and were comparable with the numbers of SRB660 probe-stained cells.

The surface fractions of SRB probe-stained cell area to total biomass area were determined (Fig. 3B) and compared with the result of the FISH direct counts. The surface fraction of the SRB probe-stained cell area was in the range of 1 to 11% with a peak at 400 to 600 μm from the surface, which was most likely due to accumulation of S^0 (see Fig. 5A).

Vertical distributions of MPN counts and potential activity. To verify the high abundance of SRB in the upper part of the biofilm detected by in situ hybridization, the vertical distributions of potential SRR, MPN counts of cultivable SRB populations, ASOR, and ANSOR were simultaneously determined (Fig. 4). Figure 4A shows that the SRR in the oxic layer was approximately 1.1 μmol cm^{-3} h^{-1} and was as high as the value at the lowest depth. However, the MPN counts decreased exponentially with depth, and the cell counts at the oxic surface layer (approximately 2×10^7 MPN cm^{-3}) were 100 times higher than the cell counts found at the deeper part of the biofilm (2×10^5 MPN cm^{-3}).

The vertical distributions of potential ASOR and ANSOR showed that the ASOR was higher in the oxic surface stratum and that the ANSOR increased with the biofilm depth (Fig. 4C). The ASOR and ANSOR were 2 and 1 orders of magnitude higher than the SRR, respectively.

Distribution of reduced inorganic sulfur compounds in the biofilm. Figure 5A represents the spatial distribution of AVS, CRS, and S^0 in a 1,200-μm-thick biofilm (a 65-day-old biofilm). Although AVS was not detectable in the surface and in the bottom of the biofilm, about 14 μmol of S $(cm^3 \text{ of AVS})^{-1}$ found at about 250 μm from the surface, at which the active H_2S production was detected by microelectrode measurements (see Fig. 6). Elemental sulfur (S^0) seemed to be the most abundant sulfur pool at all depths of the biofilm. The concentration of S^0 at about 150 μm from the surface was the highest (approximately 30 μmol of S cm^{-3}) and gradually decreased toward the bottom. The CRS concentration was below 10 μmol of S cm^{-3} throughout the biofilm, constituting a relatively small fraction of the total sulfur pools. Since elemental sulfur was never detected in the influent, S^0 accumulation was certainly due to internal reoxidation of the produced H_2S.

Figure 5B presents the profiles of total Fe and Mn concentrations in the same biofilm. The total Mn concentration was low (0.05 to 0.1 μmol cm^{-3}) throughout the biofilm. The total Fe concentration was in the range of 4.3 to 10.0 μmol cm^{-3} and was relatively constant throughout the biofilm.

Microelectrode measurements. Typical steady-state concentration profiles of O_2, H_2S, NO_3^-, NO_2^-, and pH in a biofilm

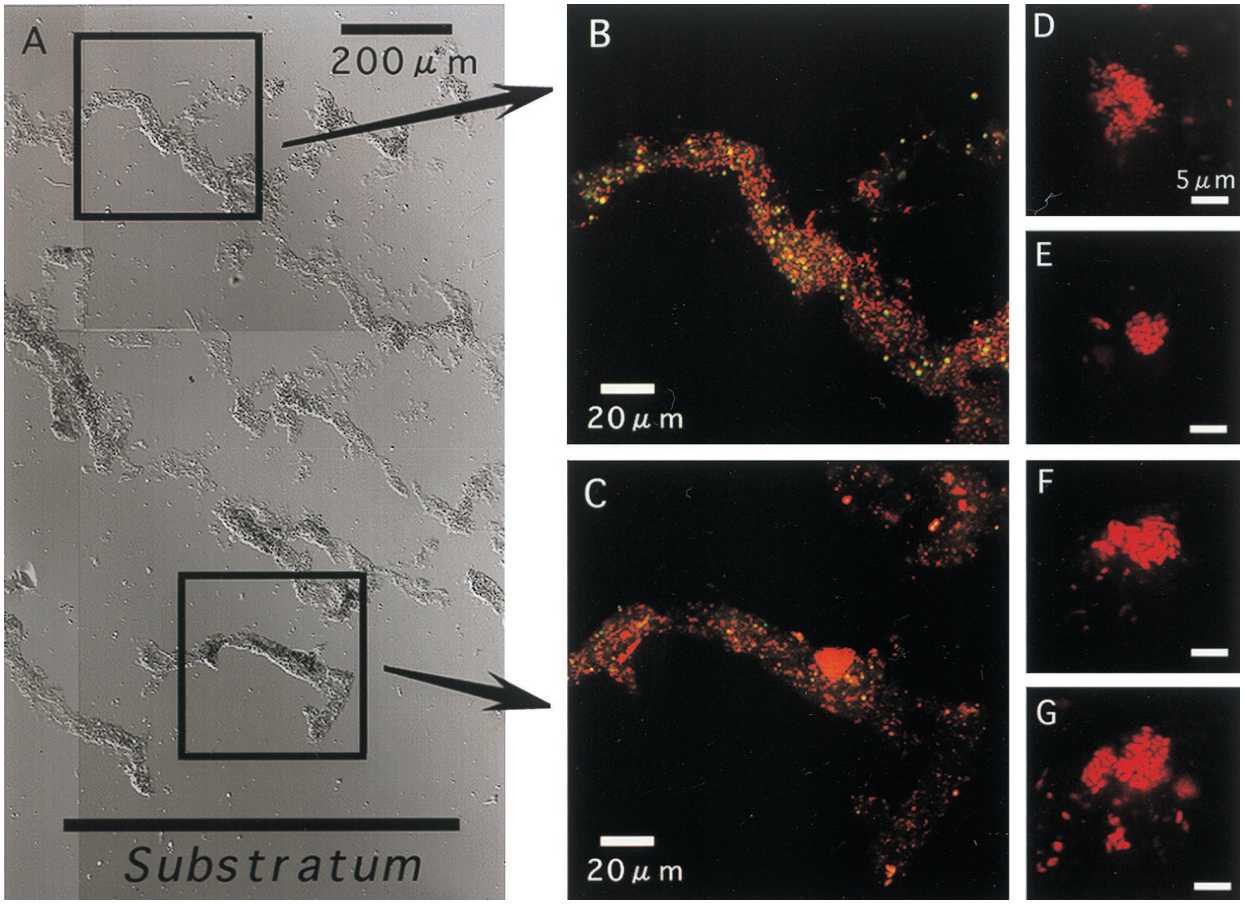

FIG. 2. In situ hybridization of vertical sections (20 μm thick) of an aerobic wastewater biofilm with TRITC-labeled SRB660 probe (specific for *Desulfobulbus* spp.). (A) Composite DIC image of the entire biofilm vertical section (scale bar = 200 μm). The biofilm thickness is about 1,500 μm. (B and C) CSLM projection images of the microscopic fields enclosed by boxes. Images were obtained by using simultaneous excitation with 488- and 543-nm lasers. Weak yellow signals were autofluorescence. (D to G) Close-up views of SRB385 probe-stained cell clusters.

incubated in the medium containing 70 μM DO, 270 μM NO_3^-, 100 μM NO_2^-, 300 μM SO_4^{2-}, and 600 μM Na-propionate are shown in Fig. 6. The concentrations of O_2, NH_4^+, SO_4^{2-}, and NO_3^- were in a range similar to those in the reactor bulk concentrations. Oxygen penetrated only about 100 μm from the surface in a biofilm approximately 1,000 μm thick, whereas NO_3^- penetrated further down, to 300 μm. Sulfide was produced in a narrow zone 150 to 300 μm below the surface at a maximum specific rate of 21 μmol of H_2S cm^{-3} h^{-1}. Below the sulfate reduction zone, a constant H_2S concentration (approximately 60 μM) was observed, indicating no net sulfide production. A possible explanation could be a carbon limitation caused by an overall depletion of carbon source in the medium during the more-than-10-h measurement and a high level of competition for the carbon source with denitrifying bacteria in the presence of NO_3^-. This was indirectly supported by the fact that sulfide production increased with increasing propionate concentrations (data not shown). A narrow sulfide oxidation zone (50 to 150 μm from the surface) was found just above the sulfate reduction zone with a maximum specific H_2S oxidation rate of 20 μmol of H_2S cm^{-3} h^{-1}, giving a total H_2S oxidation rate of 0.20 μmol of H_2S cm^{-2} h^{-1} (specific reaction rates multiplied by the depth of the reaction zone). The specific O_2 respiration rate was 11 to 19 μmol of O_2 cm^{-3} h^{-1}, giving a total consumption rate of 0.24 μmol of O_2 cm^{-2} h^{-1}. The specific NO_3^- consumption rate was 3 to 19 μmol of NO_3^- cm^{-3} h^{-1}, giving a total consumption rate of 0.59 μmol of NO_3^- cm^{-2} h^{-1}. Since the NO_2^- profile indicates that NO_2^- was produced in the anoxic biofilm stratum, the production of NO_2^- at a rate of 0.16 μmol of NO_2^- cm^{-2} h^{-1} was due to the result of nitrate reduction. The NO_2^- profiles were measured only to a depth of 150 μm, because below that sulfide induced signal drift.

DISCUSSION

Vertical distributions of SRB determined by in situ hybridization. Aerobic wastewater biofilms displayed considerable structural heterogeneity (Fig. 1). In situ spatial organization of SRB within the biofilm was successfully visualized by FISH in combination with CSLM. We found that *Desulfobulbus* spp. could be numerically important species and were consistently present in high numbers (approximately 10^8 to 10^9 cells cm^{-3}) throughout the biofilm, even in the oxic surface. They accounted for about 6 to 23% of the number of SRB385 probe-stained cells (approximately 10^9 to 10^{10} cells cm^{-3}). The relatively even distribution of SRB populations throughout the biofilm might indicate that the biofilm was grown under relatively dynamic conditions. The number of SRB obtained from the FISH analysis in this study was about 1 order of magnitude higher than the numbers of SRB in other wastewater biofilm systems (40, 42); accordingly, the SRR was higher with this factor. This is partly because the DO concentration in this study was lower than that in the other systems.

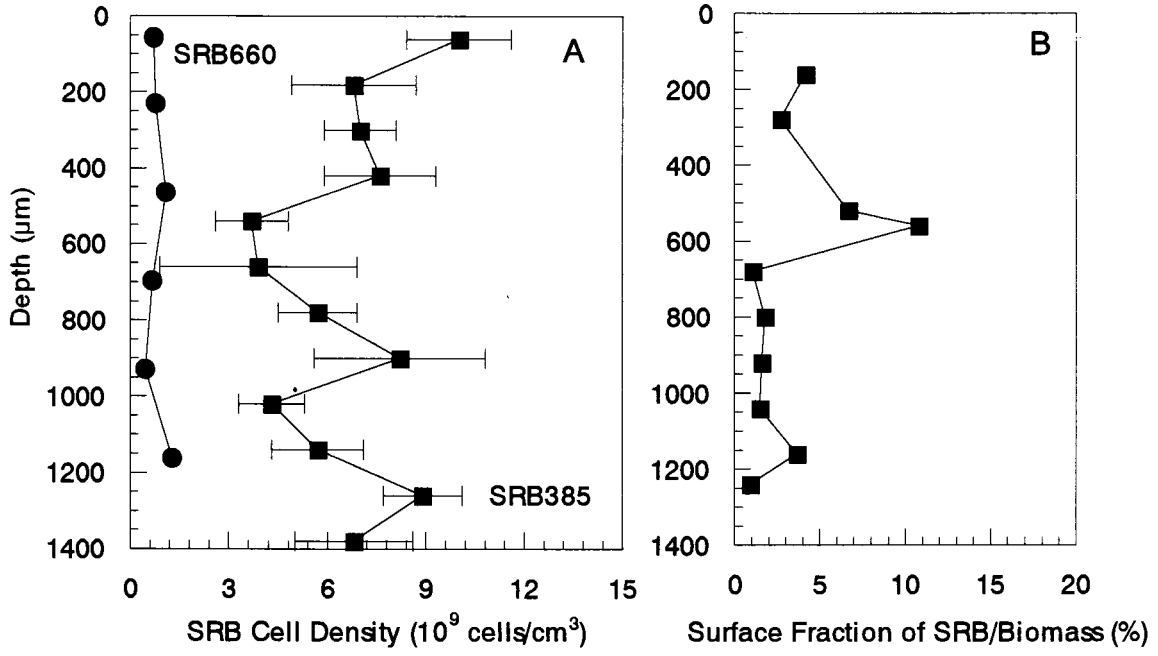

FIG. 3. Vertical distributions of SRB populations in the biofilm determined as SRB cell density (A) and surface fraction of SRB385 probe-stained cell area to the total biomass area (B). Average cell densities were determined from FISH direct cell counts along vertical transects through the biofilm after hybridization with TRITC-labeled SRB385 probe and SRB660 probe (specific for *Desulfobulbus* spp.). Error bars indicate the standard deviations of measurements. The biofilm surface is at a depth of 0 μm.

Although we have used stringent hybridization conditions and have manually counted only strongly stained cells (Fig. 2B to G), excluding autofluorescence derived from refractive detrital matters and mineral grains by using simultaneous excitation of 488- and 543-nm lasers, an exact quantitative analysis is hampered by several factors. The distinction between the autofluorescence and the true-positive cell signals was sometimes difficult to make when cells were associated with clusters

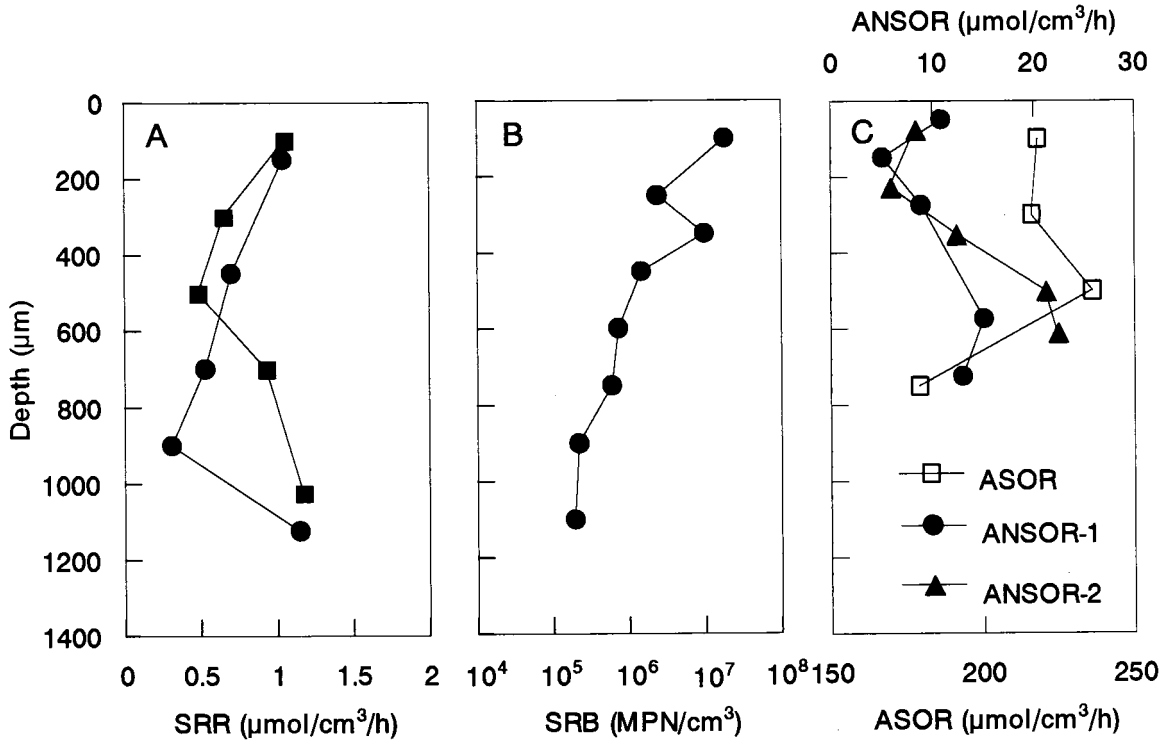

FIG. 4. Vertical distributions of potential SRRs (A), MPN counts of SRB (B), and ASORs and ANSORs (C) in the biofilm. The biofilm surface is at a depth of 0 μm.

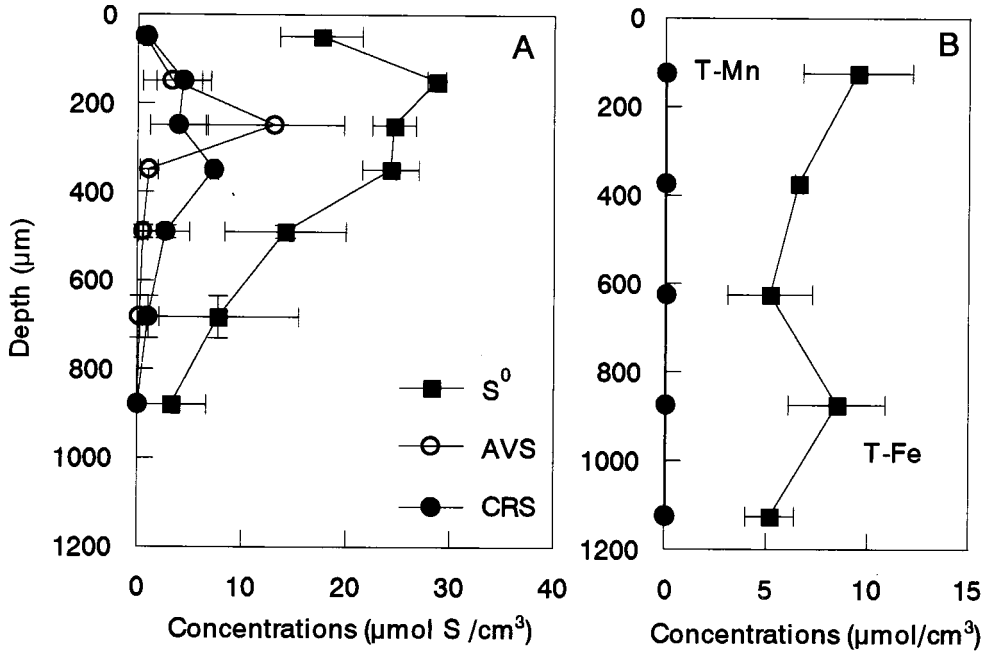

FIG. 5. Concentration profiles of reduced inorganic sulfur compounds (S^0, AVS, and CRS) (A) and total Fe and total Mn (B) in the biofilm. The biofilm surface is at a depth of 0 μm. Error bars indicate the standard deviations of measurements.

and refractive detrital matters. Thus, the cell numbers and surface fractions of SRB populations determined by FISH tend to be overestimated. For example, the higher surface fraction detected at 400 to 600 μm (Fig. 3B) was thought to be overestimated to a certain degree due to the higher concentration of elemental sulfur as shown in Fig. 5A. Furthermore, some of the oligonucleotide probes, i.e., SRB385 and SRB687, are not as specific as originally described. It is now known that the SRB385 probe is specific for sulfate reducers of the delta *Proteobacteria* and several gram-positive bacteria (e.g., *Clostridium* spp.) (3, 39). The SRB660 probe is presently known to be specific for only *Desulfobulbus* spp., and therefore the vertical profile of the probe SRB660-stained *Desulfobulbus* spp. is more reliable.

These potential experimental errors, however, do not negate the general trend of the FISH analyses. The vertical distribution of the potential SRR showed that the relatively high sulfate-reducing activity was found even in the surface biofilm, corresponding to the in situ hybridization results. This clearly suggests that a relatively high number of SRB were, indeed, present in the oxic surface zone and that their activity was sustained.

During the last few years, evidence that the anaerobic SRB are to some extent O_2 tolerant (16, 28) or are even able to oxidize reduced sulfur compounds to sulfate with O_2 or NO_3^- as the electron acceptor (9, 16) has been accumulating. A versatile metabolism of SRB, especially *Desulfobulbus* spp., with NO_3^- or even O_2 as electron acceptor (8, 9, 16, 49) could help to explain the higher abundance of SRB in the oxic surface biofilm. The anaerobic oxidation of S^0 to sulfate with oxidized metals as the electron acceptor by some SRB species and S^0 disproportionation in the absence of an electron acceptor by *Desulfobulbus propionicus* could also be a possible explanation (27). On the other hand, it is likely that the SRB present in the surface of the biofilm originated from the wastewater instead of being developed in the biofilm. Attachment of SRB cells from the wastewater to the biofilm surface is a very important process determining the SRB community structure in the biofilm. Since we did not analyze the microbial composition of the influent wastewater in this study, detailed mechanisms of development of SRB populations in the biofilm are not clear at present.

Similar observations of the higher SRR and SRB cell density in oxic environments have been reported previously in the literature (5, 21, 28). Teske et al. (45) and Santegoeds et al. (42) have found that *Desulfobulbus* and *Desulfovibrio* species were also the main SRB members in the aerobic layer of a stratified fjord and in an aerobic wastewater biofilm, respectively, underlining their ability to survive in the presence of oxygen.

Vertical distributions of MPN counts of SRB and their activity. With FISH analyses, we found 10^9 to 10^{10} SRB385 probe-stained cells per cm^3 of biofilm (including pore [void] volumes), numbers which were about 3 to 4 orders of magnitude higher than the numbers of the MPN counts. The cultivation-based enumeration of SRB by MPN apparently used a medium with propionate as sole carbon source. Most sulfate reducers such as *Desulfovibrio*, *Desulfobacter*, and *Desulfobacterium* spp. and so on were not able to grow in this medium. It is thus most likely that the MPN counts reflect only propionate-utilizing SRB species (i.e., *Desulfobulbus* spp.), which may have led to a severe underestimation of the MPN counts. The results of the MPN counts were also several orders of magnitude (10^2 to 10^4) lower than *Desulfobulbus* counts by FISH probing. Furthermore, the MPN counts decreased exponentially with depth, and the cell counts at the surface were 100 times higher than the cell counts at the base of the biofilm (Fig. 4B). This is quite different from the results of the FISH counts and the potential SRRs, which are relatively constant throughout the biofilm. This discrepancy could be explained by the fact that more *Desulfobulbus* bacteria were present in the form of densely packed clusters consisting of up to a few hundred cells in the deeper part of the biofilm than in the surface biofilm (Fig. 2), and thus, dispersion of clustered cells was not sufficiently done in the MPN counts.

Considering the total cell density of 10^{10} to 10^{11} cells per cm^3

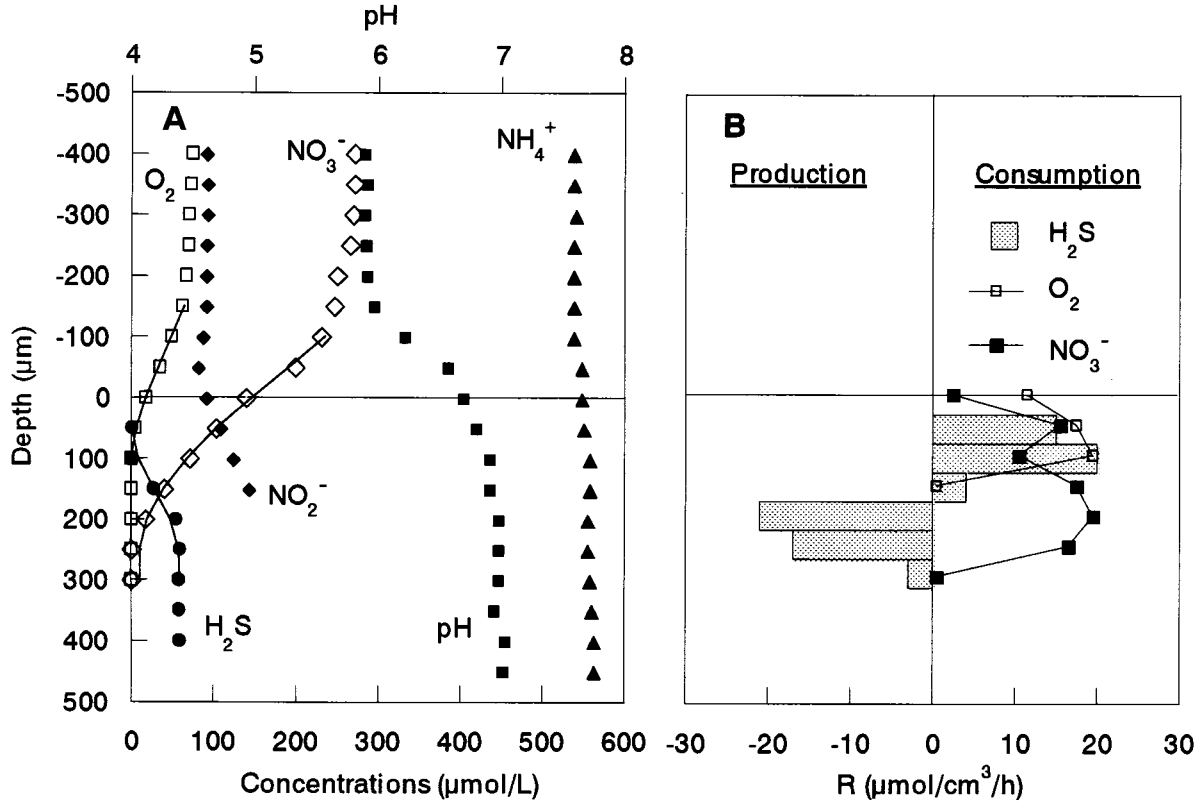

FIG. 6. Steady-state concentration profiles of O_2, NH_4^+, NO_2^-, NO_3^-, H_2S, and pH in the aerobic wastewater biofilm incubated in DO-controlled (DO = approximately 70 μM) medium with 600 μM Na-propionate, 550 μM NH_4^+, 270 μM NO_3^-, 300 μM SO_4^{2-}, and 100 μM NO_2^- (A) and the spatial distribution of the estimated specific consumption and production rates of O_2, NO_3^-, and H_2S (B). The points are measured mean values of measurements in triplicate. The solid lines are the best fits from the model to calculate the specific consumption and production rates of O_2, NO_3^-, and H_2S. The biofilm surface is at a depth of 0 μm. R, rate.

of a similar biofilm (34), the relative percentage of SRB cells is on the order of 1 to 10%. This order is in the range of the surface fraction of SRB385 probe-stained cells obtained in this study (Fig. 3B). To evaluate the SRB enumeration efficiency of the FISH counts, the specific SRRs were calculated. The specific SRRs in this biofilm were on the order of 10^{-15} mol of SO_4^{2-} $cell^{-1}$ day^{-1}. This rate is in the range of the previously reported specific SRRs of pure cultures on H_2, lactate, or pyruvate: 2×10^{-16} to 5×10^{-14} mol of SO_4^{2-} $cell^{-1}$ day^{-1} (19).

The measurement of potential SRRs in the batch experiment showed lower rates (0.3 to 1.1 μmol of H_2S cm^{-3} h^{-1}) than the rates calculated from microprofile data (in the range of 3 to 21 μmol of H_2S cm^{-3} h^{-1}) (Fig. 6). This difference can be explained by deterioration of sulfate reduction activity during the microslicing and homogenization processes and by cycling use of the produced H_2S and SO_4^{2-}. The measurement of potential SRRs used the same medium as the MPN counts with propionate as sole carbon source, and the concentration of propionate was very high compared with the actual concentrations. This may have led to a severe underestimation.

The SRRs calculated from the H_2S microprofile were prone to relatively large errors, which limited an exact quantitative comparison of the in situ activity. First, the measured concentration profiles presented in Fig. 6 are not profiles that actually occurred under growth conditions in the biofilm reactor, because, for example, the reactor hydrodynamics were different. Flow velocities above the biofilm in the microelectrode measurements were in the range of 2 to 3 cm s^{-2}, which is lower than a peripheral speed of ca. 14 cm s^{-1} when the disk rotational speed of the RDR is 14 rpm. Thus, the thickness of the diffusion boundary layer is expected to be thinner under the actual growth conditions, which increases substrate fluxes into the biofilm and consequently affects rates and locations of successive respiratory processes. Second, the wastewater biofilms displayed considerable structural heterogeneity, as shown in Fig. 1. However, the influence of the biofilm heterogeneity on diffusion coefficients was not taken into account when the specific reaction rates were calculated, and thus constant diffusion coefficients were used throughout the biofilm. Third, the S^{2-} sensors used in this study are sensitive to oxygen, so that some overlaps of the O_2 and H_2S profiles occur. Thus, the H_2S profile in the zone where O_2 and H_2S coexist may not be reliable.

The average in situ SRR determined by the microelectrode measurement was 13.0 ± 6.6 μmol of H_2S cm^{-3} h^{-1}, which is lower than the maximum specific SRRs without substrate limitation reported in previous studies of an anaerobic SRB biofilm (approximately 56 to 93 μmol of H_2S cm^{-3} h^{-1} at 20°C) (30) and of a pure-cultured *Desulfovibrio desulfuricans* biofilm (approximately 484 μmol of SO_4^{2-} cm^{-3} h^{-1} at 35°C) (35). However, the rate is higher than the rates reported in previous microsensor studies of other wastewater biofilm systems (0.3 to 1.6 μmol of H_2S cm^{-3} h^{-1}) (22, 40, 42) and of marine sediments (approximately 0.1 to 4 nmol of H_2S cm^{-3} h^{-1}) (19, 21). The higher SRRs in this study than in the other biofilm systems were due primarily to the higher abundance of SRB populations and the lower DO concentration in the bulk water.

Oxygen consumption. An approximate budget of the oxygen consumption was estimated from the vertical distributions of the specific consumption rates of O_2, H_2S, and NO_3^- calculated from the microprofiles (Fig. 6B). The H_2S profile over-

lapped with the O_2 and NO_3^- profiles, indicating that the produced H_2S was aerobically and anaerobically oxidized in the biofilm. Sulfide denitrifiers, e.g., *Thiobacillus denitrificans*, preferentially utilize O_2 over NO_3^- as electron acceptor in the presence of O_2 and NO_3^-. Therefore, we assumed that NO_3^- was utilized by sulfide denitrifiers after O_2 was completely depleted in the zone where the H_2S profile overlaps with the O_2 and NO_3^- profiles. We also assumed that the main product of both aerobic and anaerobic H_2S oxidation is SO_4^{2-}. Taking into account the fact that oxidation of 1 mol of H_2S to SO_4^{2-} requires 2 mol of O_2 for aerobic oxidation and 4 mol of NO_3^- for anaerobic oxidation (i.e., $4NO_3^- + H_2S \rightarrow 4NO_2^- + SO_4^{2-} + 2H^+$), the fraction of O_2 consumption for H_2S oxidation was determined within each measurement step and integrated throughout the reaction zone (Fig. 6B). As a result, a large fraction (up to 76%) of total O_2 consumption was due to the reoxidation of H_2S. Thus, sulfate reduction is as important as aerobic respiration in this biofilm. Based on the total H_2S consumption rate (ca. 0.20 μmol of H_2S cm^{-2} h^{-1}) determined from the H_2S profile (at the point of the steepest gradient) and the integrated H_2S oxidation rate with NO_3^- (ca. 0.11 μmol of H_2S cm^{-2} h^{-1}) determined from the specific consumption rates of O_2, NO_3^-, and H_2S, approximately 55% of the sulfide produced was anaerobically reoxidized to SO_4^{2-}. However, if more-reduced sulfur compounds such as S^0 are formed as the product, the H_2S reoxidation becomes less important. Thus, it should be noted that the calculations indicate the upper limits of SRB contribution.

Santegoeds et al. (42) have reported that H_2S reoxidation accounted for up to 70% of total oxygen consumption in aerobic biofilms in the absence of NO_3^-. Lower potential contributions (10 to 50%) of H_2S reoxidation were found for gravity sewer biofilms (32), for an aerobic trickling filter biofilm (22), and for wastewater biofilms on rotating biological contactors (25).

Sulfide oxidation. To investigate the potential sulfide oxidative pathways, average turnover times of O_2, NO_3^-, and H_2S in the H_2S-oxidizing zones were calculated as the ratio of the average concentration in the H_2S oxidation zone to the average reaction rate (both determined from microprofiles) as described by Kuhl and Jorgensen (22). These turnover times were extremely short (less than a minute) compared with possible spontaneous chemical reaction of O_2 and H_2S. The timescale of the O_2-H_2S reaction at wastewater temperature has been reported to be in the range of minutes to several hours (6, 17). Thus, the observed aerobic and anaerobic oxidation of H_2S was mediated mainly by microbial reactions and instantaneous reaction with metal ions. However, the latter reaction is less important (see below). Accordingly, SRRs in biofilms can be reliably measured in situ only by microelectrodes. It should be noted that the measured ASOR and ANSOR were about 1 to 2 orders of magnitude higher than the SRRs (Fig. 4C). Therefore, sulfate reduction was probably the rate-limiting step in the series of sulfur transformations in the biofilm.

Sulfur pools in biofilms. So far, measurements of inorganic reduced sulfur compounds (i.e., sulfur pools) in wastewater biofilm systems are scarce. Nielsen et al. (31) have reported that the maximum total sulfur pool in an alternating oxic and anoxic biofilm system attached on the metal coupon was 157 μmol of S cm^{-3}, which consisted mainly of AVS (FeS) and CRS (FeS_2). Compared with this figure, the total S pool in the biofilm in the present study was rather small (approximately 23 μmol of S cm^{-3}). However, it is important to note that elemental sulfur (S^0) was an important intermediate of the sulfide reoxidation in such thin wastewater biofilms, which accounted for about 75% of the total S pool. S^0 could be produced by both geochemical and biological H_2S oxidation processes. We speculate that the dominance of S^0 at the surface biofilm (Fig. 5A) resulted from the high SRR followed by the intensive microbial sulfide reoxidation. The importance of the dominance of S^0 in the biofilm is that S^0 disproportionation is thermodynamically as favorable and important a process as sulfide production. High concentrations of S^0 were found in the zone where the SRR was high according to the microprofiles (Fig. 6). This may suggest that a part of sulfide production is not due to sulfate reduction by SRB. S^0 is also very corrosive to wastewater treatment facilities and could be reduced to H_2S and/or oxidized to SO_4^{2-} by some SRB and other species.

The reliability of the spatial distribution of AVS, CRS, and S^0 in the biofilm was evaluated because of such small sample volumes and losses from exposure of the samples to oxygen. We measured concentrations of AVS, CRS, and S^0 in an entire biofilm and in the same biofilm samples apportioned into three layers by the Microslicer. Then the total amount of AVS, CRS, and S^0 in the entire intact biofilm was compared with the sum of the concentrations of each biofilm section. The sums of AVS, CRS, and S^0 concentrations of the sectioned biofilm samples were 68, 114, and 75%, respectively. Thus, the concentration profiles of AVS, CRS, and S^0 in the biofilm (Fig. 5A) should be read with this factor being taken into account.

Contribution of an internal Fe-sulfur cycle in the overall sulfur cycle. The H_2S profile showed that H_2S diffused up to the very surface of the biofilm, indicating a relatively high in situ SRR (Fig. 6A). A comparison of the high SRRs and the slow accumulation of total reduced sulfur compounds in the biofilm indicated that intensive reoxidation of H_2S must have taken place. The average in situ SRR determined by the microelectrode measurement (Fig. 6) was approximately 13.0 ± 6.6 μmol of H_2S cm^{-3} h^{-1}. The mean accumulation rate of total reduced sulfur compounds in the biofilm was approximately 0.021 to 0.031 μmol of S cm^{-3} h^{-1} (33). Thus, only up to 0.3% of the produced H_2S was retained as FeS, FeS_2, and S^0, which must be regarded as an electron sink of aerobic biofilms. The remaining 99.7% was reoxidized to sulfate in the oxic and/or anoxic zone, indicating that the contribution of an internal Fe-sulfur cycle in the overall sulfur cycle is insignificant. Therefore, the role of AVS can be regarded as an important electron carrier from the deeper anoxic sulfate reduction zone to the oxic-anoxic interface. The degree of reoxidation of the H_2S produced in marine sediments was about 80 to 95% (20, 21), indicating that oxidized iron minerals (i.e., the Fe-S cycle) play a more important role than they do in wastewater biofilm systems. This can be explained by a shorter diffusion distance and a much higher SRR, which is due to the higher influx of organic matter and the higher abundance of SRB populations in wastewater biofilm systems.

Concluding remarks. The results of the combined study of in situ hybridization with the specific phylogenetic probes and microelectrode measurements provided a more detailed picture of the abundance, the spatial distribution, and the activity of SRB populations in the aerobic wastewater biofilm. In addition, a cross-evaluation of the FISH and microelectrode data was performed by comparing them with culture-based approaches and biogeochemical measurements. In situ hybridization revealed that a relatively high abundance (approximately 10^9 to 10^{10} cells per cm^3) of SRB was present throughout the biofilms, even in the oxic surface layer. Probe SRB660-stained *Desulfobulbus* was found to be a numerically important member of SRB populations (approximately 10^8 to 10^9 cells per cm^3). The biogeochemical measurements showed that elemental sulfur (S^0) was an important intermediate of the sulfide reoxidation in thin wastewater biofilms, which accounted for

75% of the total S pool. The contribution of an internal Fe-sulfur cycle to the overall sulfur cycle in aerobic wastewater biofilms was insignificant.

ACKNOWLEDGMENTS

We gratefully appreciate Dirk deBeer, Max Planck Institute for Marine Microbiology, Bremen, Germany, and Per H. Nielsen, Environmental Engineering Laboratory, Aalborg University, Aalborg, Denmark, for valuable discussions and critical review of the manuscript.

This research has been supported by the CREST (Core Research for Evolutional Science and Technology) of Japan Science and Technology Corporation (JST) and by a grant-in-aid (no. 09750627) for Developmental Scientific Research from the Ministry of Education, Science and Culture of Japan.

REFERENCES

1. **Amann, R. I.** 1995. *In situ* identification of micro-organisms by whole-cell hybridization with rRNA-targeted nucleic acid probes, p. 1–15. *In* A. D. L. Akkerman, J. D. van Elsas, and F. J. de Bruijn (ed.), Molecular microbial ecology manual. Kluwer Academic Publishers, Dordrecht, The Netherlands.
2. **Amann, R. I., L. Krumholz, and D. A. Stahl.** 1990. Fluorescent-oligonucleotide probing of whole cells for determinative, phylogenetic, and environmental studies in microbiology. J. Bacteriol. **172:**762–770.
3. **Amann, R. I., J. Stromley, R. Devereux, R. Key, and D. A. Stahl.** 1992. Molecular and microscopic identification of sulfate-reducing bacteria in multispecies biofilms. Appl. Environ. Microbiol. **58:**614–623.
4. **Andrussow, L.** 1969. Diffusion, p. 513–727. *In* Landolt-Bornstein Zahlenw. Funkt., vol. II/5a. Springer-Verlag, Berlin, Germany.
5. **Canfield, D. E., and D. J. Des Marais.** 1991. Aerobic sulfate reduction in microbial mats. Science **251:**1471–1473.
6. **Chen, K. Y., and J. C. Morris.** 1972. Kinetics of oxidation of aqueous sulfide by O_2. Environ. Sci. Technol. **6:**529–537.
7. **Cline, J. D.** 1969. Spectrophotometric determination of hydrogen sulfide in natural waters. Limnol. Oceanogr. **14:**454–458.
8. **Dalsgaard, T., and F. Bak.** 1994. Nitrate reduction in a sulfate-reducing bacterium, *Desulfovibrio desulfuricans*, isolated from rice paddy soil: sulfide inhibition, kinetics, and regulation. Appl. Environ. Microbiol. **60:**291–297.
9. **Dannenberg, S., M. Kroder, W. Dilling, and H. Cypionka.** 1992. Oxidation of H_2, organic compounds and inorganic sulfur compounds coupled to reduction of O_2 or nitrate by sulfate-reducing bacteria. Arch. Microbiol. **158:**93–99.
10. **deBeer, D., A. Schramm, C. M. Santegoeds, and M. Kühl.** 1997. A nitrite microsensor for profiling environmental biofilms. Appl. Environ. Microbiol. **63:**973–977.
11. **deBeer, D., and J.-P. R. A. Sweerts.** 1989. Measurements of nitrate gradients with an ion selective microelectrode. Anal. Chem. Acta **219:**351–356.
12. **deBeer, D., and J. C. van den Heuvel.** 1988. Gradients in immobilized biological systems. Anal. Chem. Acta **213:**259–265.
13. **deBeer, D., and J. C. van den Heuvel.** 1989. Response of ammonium-selective microelectrodes based on the neutral carrier nonactin. Talanta **35:**728–730.
14. **deBeer, D., J. C. van den Heuvel, and S. P. P. Ottengraf.** 1993. Microelectrode measurements of the activity distribution in nitrifying bacterial aggregates. Appl. Environ. Microbiol. **59:**573–579.
15. **Devereux, R., M. D. Kane, J. Winfrey, and D. A. Stahl.** 1992. Genus- and group-specific hybridization probes for determinative and environmental studies of sulfate-reducing bacteria. Syst. Appl. Microbiol. **15:**601–609.
16. **Dilling, W., and H. Cypionka.** 1990. Aerobic respiration in sulfate-reduction bacteria. FEMS Microbiol. Lett. **71:**123–128.
17. **Eary, L. E., and J. A. Schramke.** 1990. Rates of inorganic oxidation reactions involving dissolved oxygen, p. 379–396. *In* D. C. Melchior and R. L. Basset (ed.), Chemical modeling of aqueous systems II. American Chemical Society, Washington, D.C.
18. **Fossing, H., and B. B. Jorgensen.** 1989. Measurement of bacterial sulfate reduction in sediments: evaluation of a single-step chromium reduction method. Biogeochemistry **8:**205–222.
19. **Jorgensen, B. B.** 1978. A comparison of methods for the quantification of bacterial sulfate reduction in coastal marine sediments. III. Estimation from chemical and bacteriological field data. Geomicrobiol. J. **1:**49–64.
20. **Jorgensen, B. B.** 1982. Mineralization of organic matter in the sea bed—the role of sulphate reduction. Nature (London) **296:**643–645.
21. **Jorgensen, B. B., and F. Bak.** 1991. Pathways and microbiology of thiosulfate transformations and sulfate reduction in a marine sediment (Kattegat, Denmark). Appl. Environ. Microbiol. **57:**847–856.
22. **Kuhl, M., and B. B. Jorgensen.** 1992. Microsensor measurements of sulfate reduction and sulfide oxidation in compact microbial communities of aerobic biofilms. Appl. Environ. Microbiol. **58:**1164–1174.
23. **Lee, W., Z. Lewandowski, S. Okabe, W. G. Characklis, and R. Avci.** 1993. Corrosion of mild steel underneath aerobic biofilms containing sulfate-reducing bacteria. Part I: at low bulk oxygen concentration. Biofouling **7:**197–216.
24. **Lee, W., Z. Lewandowski, M. Morison, W. G. Characklis, R. Avci, and P. H. Nielsen.** 1993. Corrosion of mild steel underneath aerobic biofilms containing sulfate-reducing bacteria. Part II: at high bulk oxygen concentration. Biofouling **7:**217–239.
25. **Lens, P. N., M.-P. De Poorter, C. C. Cornenberg, and W. H. Verstraete.** 1995. Sulfate reducing and methane producing bacteria in aerobic wastewater treatment systems. Water Res. **29:**871–880.
26. **Lorenzen, J., L. H. Larsen, T. Kjar, and N. P. Revsbech.** 1998. Biosensor detection of the microscale distribution of nitrate, nitrate assimilation, nitrification, and denitrification in a diatom-inhabited freshwater sediment. Appl. Environ. Microbiol. **64:**3264–3269.
27. **Lovley, D. R., and E. J. P. Phillips.** 1994. Novel processes for anaerobic sulfate production from elemental sulfur by sulfate-reducing bacteria. Appl. Environ. Microbiol. **60:**2394–2399.
28. **Marschall, C., P. Frenzel, and H. Cypionka.** 1993. Influence of oxygen on sulfate reduction and growth of sulfate-reducing bacteria. Arch. Microbiol. **159:**168–173.
29. **Millero, F. J., and J. P. Hershey.** 1989. Thermodynamics and kinetics of hydrogen sulfide in natural waters, p. 282–313. *In* E. S. Saltzman and W. J. Cooper (ed.), Biogenic sulfur in the environment. American Society for Microbiology, Washington, D.C.
30. **Nielsen, P. H.** 1987. Biofilm dynamics and kinetics during high-rate sulfate reduction under anaerobic conditions. Appl. Environ. Microbiol. **53:**27–32.
31. **Nielsen, P. H., W. Lee, Z. Lewandowski, M. Morison, and W. G. Characklis.** 1993. Corrosion of mild steel in an alternating oxic and anoxic biofilm system. Biofouling **7:**267–284.
32. **Norsker, N. H., P. H. Nielsen, and T. Hvitved-Jacobsen.** 1995. Influence of oxygen on biofilm growth and potential sulfate reduction in gravity sewer biofilm. Water Sci. Technol. **31:**159–167.
33. **Okabe, S., and T. Itoh.** 1998. Unpublished data.
34. **Okabe, S., K. Hirata, Y. Ozawa, and Y. Watanabe.** 1996. Spatial microbial distributions of nitrifiers and heterotrophs in mixed population biofilms. Biotechnol. Bioeng. **50:**24–35.
35. **Okabe, S., P. H. Nielsen, W. L. Jones, and W. G. Characklis.** 1995. Rate and stoichiometry of microbial sulfate reduction by *Desulfovibrio desulfuricans* in biofilms. Biofouling **9:**63–83.
36. **Okabe, S., H. Satoh, and Y. Watanabe.** 1999. In situ analysis of nitrifying biofilms as determined by in situ hybridization and the use of microelectrodes. Appl. Environ. Microbiol. **65:**3182–3191.
37. **Postgate, J. R.** 1984. The sulphate-reducing bacteria, 2nd ed. Cambridge University Press, Cambridge, United Kingdom.
38. **Rabus, R., M. Fukui, H. Wilkers, and F. Widdel.** 1996. Degradative capacities and 16S rRNA-targeted whole-cell hybridization of sulfate-reducing bacteria in an anaerobic enrichment culture utilizing alkylbenzenes from crude oil. Appl. Environ. Microbiol. **62:**3605–3613.
39. **Ramsing, N. B., H. Fossing, T. G. Ferdelman, F. Andersen, and B. Thamdrup.** 1996. Distribution of bacterial populations in a stratified fjord (Mariager Fjord, Denmark) quantified by in situ hybridization and related to chemical gradients in the water column. Appl. Environ. Microbiol. **62:**1391–1404.
40. **Ramsing, N. B., M. Kuhl, and B. B. Jorgensen.** 1993. Distribution of sulfate-reducing bacteria, O_2, and H_2S in photosynthetic biofilms determined by oligonucleotide probes and microelectrodes. Appl. Environ. Microbiol. **59:**3840–3849.
41. **Revsbech, N. P., and B. B. Jorgensen.** 1986. Microelectrodes: their use in microbial ecology. Adv. Microb. Ecol. **9:**293–352.
42. **Santegoeds, C. M., T. G. Ferdelman, G. Muyzer, and D. deBeer.** 1998. Structure and functional dynamics of sulfate-reducing populations in bacterial biofilms. Appl. Environ. Microbiol. **64:**3731–3739.
43. **Schramm, A., L. H. Larsen, N. P. Revsbech, N. B. Ramsing, R. Amann, and K.-H. Schleifer.** 1996. Structure and function of a nitrifying biofilm as determined by in situ hybridization and the use of microelectrodes. Appl. Environ. Microbiol. **62:**4641–4647.
44. **Schramm, A., D. deBeer, M. Wagner, and R. Amann.** 1998. Identification and activities in situ of *Nitrosospira* and *Nitrospira* spp. as dominant populations in a nitrifying fluidized bed reactor. Appl. Environ. Microbiol. **64:**3480–3485.
45. **Teske, A., C. Wawer, G. Muyzer, and N. B. Ramsing.** 1996. Distribution of sulfate-reducing bacteria in a stratified fjord (Mariager Fjord, Denmark) as evaluated by most-probable-number counts and denaturing gradient gel electrophoresis of PCR-amplified ribosomal DNA fragments. Appl. Environ. Microbiol. **62:**1405–1415.
46. **Tuovinen, O. H., and D. P. Kelly.** 1973. Studies on the growth of *Thiobacillus ferrooxidans*. Arch. Mikrobiol. **88:**285–298.
47. **Wagner, M., R. I. Amann, P. Kampfer, B. Assmus, A. Hartmann, P. Hutzler, N. Springer, and K.-H. Schleifer.** 1994. Identification and *in situ* detection of Gram-negative filamentous bacteria in activated sludge. Syst. Appl. Microbiol. **17:**405–417.
48. **Wagner, M., B. Assmus, A. Hartmann, P. Hutzler, and R. I. Amann.** 1994. *In situ* analysis of microbial consortia in activated sludge using fluorescently labeled, rRNA-targeted oligonucleotide probes and confocal scanning laser microscopy. J. Microsc. **176:**181–187.
49. **Widdel, F., and N. Pfennig.** 1982. Studies on dissimilatory sulfate-reducing bacteria that decompose fatty acids. II. Incomplete oxidation of propionate by *Desulfobulbus propionicus* gen. nov., sp. nov. Arch. Microbiol. **131:**360–365.